Experimental Investigation and Mathematical Modelling of a Natural Convection Solar Tunnel Dryer

Sam Cherotich and Isaac N. Simate

Abstract - The purpose of this study was to investigate the performance of a natural convection solar tunnel fruit dryer and to determine an appropriate thin layer model to predict the drying. The dryer comprised of three major units: a solar collector unit, a drying unit and a bare flat-plate chimney. To investigate its performance, six sets of drying experiments with mango as the product, were carried out at the University of Zambia, Department of Agricultural Engineering under natural conditions and the following parameters were recorded: the drying time, air temperature, relative humidity, solar irradiance and air velocity. The solar irradiance varied between 470 and 1070 W m^{-2}, while air temperature of up to 70 °C was recorded at the collector unit. Ambient relative humidity varied between 11.95 and 29.67 % and was lowered by over 50 % in the dryer. With relatively low air velocities, the buoyant pressure ranged from 0.1530 to 0.3016 N m^{-2}. Under these conditions, mango with an initial moisture content of 80 % (w.b.) was dried to between 13 and 14 % (w.b.) in 11 hours. To find an appropriate thin layer model, the moisture content results were transformed to moisture ratio and fitted into 12 common thin layer models in literature using the MatlabR2011b curve fitting tool. The best model was determined based on three statistical parameters: R^2, SSE and RMSE. Midilli-Kucuk model was found to be the best model with R^2, SSE and RMSE of 0.9959, 0.004634, and 0.01758 respectively.

Key words: Chimney, Natural convection, Solar Drying, Thin layer.

1 INTRODUCTION

AMONG various fruits, mango is one of the major tropical fruits worldwide with about 98 % total production in developing countries and 80 % import trade from developed countries [1]. Besides the availability of fruits such as citrus, papaya, banana and avocado, mango is a major fruit tree in Zambia. Due to its fresh sweet tasty aroma, mango is mostly consumed in its fresh state although several other mango products are available in the markets. Among them include; dehydrated mango, mango juice and nectar, mango jam and chutney.

Mango dehydration involves reducing the initial moisture content to safe and desirable levels and this requires energy. Solar energy among other energies has been harnessed for fruit drying via open sun drying (OSD) and solar drying. The fundamental difference between the two is use of equipment by the latter. OSD is marked by some major short falls which include; exposure of the product to aerosols, insects, rain, and animals. These shortfalls immensely increase the chances for contamination, spoilage and product losses. Solar dryers have emerged over the years and have curbed down most of the short falls of OSD.

Based on the air heating mode, solar dryers may be placed into three broad categories and these include; direct-mode dryers, indirect-mode dryers and mixed-mode dryers [2]. For the direct-mode, the product is contained in the air heating unit such that the solar radiation penetrating a transparent cover heats both the product and the air. For the indirect-mode type, there is a distinct air heating unit and a drying unit. Air is preheated before drying the product in the drying unit. Finally, the mixed-mode dryers have the air heated in two stages, first, at the air heating unit and secondly, at the product drying unit. According to the air heating mode, solar tunnel dryers may be placed under the category of mixed-mode dryers.

Fruit solar drying is normally done in thin layers aiding the drying rate but most importantly, use of the thin layer equations to represent the drying phenomena is made possible. Several thin layer drying studies on fruits and vegetables are available in literature. Goyal, et al. [3] studied raw mango, Toğrul and Pehlivan [4] studied apricots, green paper by Akpinar and Bicer [5], Akpinar, et al. [6] studied parsley leaves, and hot chilli by Hossain and Bala [7] among others. Most of the literature in thin layer drying have focused on forced convection drying, however, forced convection drying systems require a fan system and a PV module or an alternative source of power to drive the fan.

- *Sam Cherotich holds a BSc. Degree in Agricultural Engineering from Makerere University, P.O. Box 7062, Kampala, Uganda. Presently, he is pursuing a MEng-Agricultural Engineering under the METEGA–intra-ACP scholarship funded by the European Union at the Department of Agricultural Engineering, University of Zambia, P.O. Box 32379, Lusaka, Zambia. Email Address: samchero@gmail.com*
- *Isaac N. Simate holds a PhD in Solar Drying from the University of Newcastle upon Tyne, U.K., MSc in Food Technology (Process Engineering Option) from the University of Reading, U.K. Email Address: isaac.simate@unza.zm.*

Most rural areas in developing countries such as Zambia lack access to grid electricity while areas with access are prone to moderate to severe load shading limiting the viability of a grid powered fan in an active solar drying system. By harnessing solar energy using a solar PV module, a solar powered fan in such areas could be a good option for active solar drying. Use of a solar PV module to power a fan in an active solar dryer however has some downsides. These include among others; high initial cost and high chances of theft of the PV module especially if the dryer is to be operated in an area remote from close monitoring.

Passive solar dryers or natural convection systems compared to active solar dyers tend to be relatively cheaper to operate and maintain [8]. However, chimneys in natural convection systems especially the bare flat-plate type have a relatively low thermal efficiency [9].

With reference to the above literature, the objective of this study was to carry out an experimental investigation of a natural convection solar tunnel dryer and to establish an appropriate thin layer model under Zambian conditions.

2 MATERIALS AND METHODS

This study was conducted at the field station of the Department of Agricultural Engineering, University Zambia (Latitude15.3°S; Longitude 28.3°E). Drying experiments were done between October and November 2015 which were generally dry months and a period when mango was ready for harvest. The drying experiments were conducted as described below. The first experiment was done to determine the initial moisture content of mango. Ripe mangoes were locally acquired from the markets and the initial moisture content determined using the standard AOAC method [10]. After determining the initial moisture content, the solar drying experiments were conducted in the experimental set-up shown in figure 1.

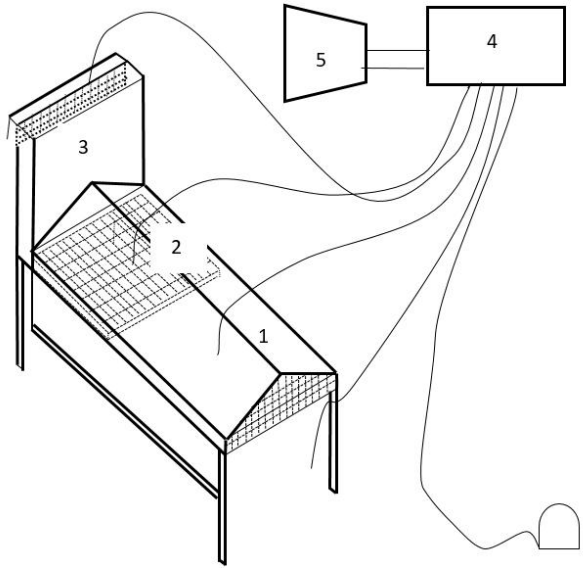

Fig.1. Schematic diagram of the solar tunnel dryer and components: (1) collector unit, (2) drying unit, (3) bare flat- plate chimney Unit, (4) Data logger and (5) Computer

2.1 Description of the dryer and its mode of operation

The solar tunnel dryer shown in figure 1 consists of three major components: (1) collector unit, (2) drying unit and (3) bare flat-plate chimney unit. The collector unit absorber plate made from a Galvanized Iron (GI) sheet and dimensions, 1.0 m× 0.75 m (L× W) was painted black using mat black paint to absorb much of the incident solar radiation. The collector and the drying units were covered by a transparent 200 µm polyethylene sheet to allow the solar radiation in to the dryer to heat the air.

In operation, the dryer was oriented in a North-South direction as suggested by Brenndorfer, et al. [11] and because of the solar radiation penetrating the transparent cover, the air entering the collector unit and the drying unit was heated through convective heating. This increases the capacity of the air to remove moisture from the product in the drying unit whose dimensions were 1.0 m × 0.75 m (L× W). The drying unit was mounted with a removable wire mesh tray which was laid with a black plastic square net. The purpose of the black plastic net was to hold the sliced product spread over it in thin layers such that heated air from the collector unit flows over the product.

The heated air causes heat and mass transfer to occur between the air and product resulting in to drying of the product. To minimize heat losses at the collector and drying units, the base and sides of these units were stuck with 20 mm Styrofoam sheets using glue.

To compensate for air flow in the dryer through the natural convection process, a bare flat-plate chimney unit made from a 0.3 mm GI sheet with dimensions 0.75 m × 0.75 m (L× W) and having an air channel of 0.1 m was mounted vertically at the end of the drying unit. The chimney surface receiving the solar radiation was painted black to absorb much of the incident solar radiation such that air leaving the drying unit was re-heated convectively to ensure its temperature was above ambient.

Re-heating the air from the drying unit causes a difference in air densities between the ambient air and air inside the dryer. This difference in air densities generates a buoyant pressure which drives air flow [8].

Supporting the dryer were 4 dryer legs 0.6 m above the ground surface and were detachable like all the other units of the dryer. The ability to detach the components from one another is one notable aspect of this dryer because it allowed easy assembly and re-assembly handy for transportation.

2.2 Experimental set-up

The experimental setup of the dryer and the recording equipment is shown in figure 1. A multi probe Campbell scientific Inc data logger (model: CR 1000) was connected to the solar tunnel dryer to record the air temperatures, relative humidity and solar radiation.

The temperature probes were thermocouple type (model: 108 – L), capable of temperature ranges between -5 and + 95 °C at an accuracy of ± 0.01 °C. The probes were connected to take the air temperature at the following points: the collector unit exit (T_c), the drying unit exit (T_d), the chimney exit (T_{ch}) and outside the dryer (T_{am}).

The air relative humidity at the following points: the collector unit (RH_c), the drying unit (RH_d) and outside the dryer (RH_{am}) were recorded using a temperature and relative humidity probe (model: HMP60-L). The relative humidity probe was capable of measuring temperature and humidity ranges of -40 to 60 °C and 0 and 100 % respectively.

The solar irradiance was recorded by a pyranometer (model: CMP6-L) while the air velocity was measured using a digital air flow meter (model: TES 1340) having an accuracy of ± 0.01 m s^{-1} for air velocities between 0 and 30 m s^{-1}. Connected to the data logger was a computer to display and retrieve the recorded readings from the data logger.

2.3 Drying procedure in the solar tunnel dryer

Mango was cleaned, peeled and sliced into 5 mm thickness. Three sliced samples each of 100 g were weighed from a digital weighing balance (model: PE 3000) with a weighing accuracy of ±0.1 g. The weighed samples were spread on 3 square black plastic nets and loaded on the wire tray (Area: 0.69 m^2) located in the drying unit. The rest of the tray area lain by a similar black plastic net was filled with a thin layer of sliced mango. At full capacity, the drying unit could carry up to 1.8 kg of sliced mango, hence a loading density of 2.5 kg m^{-2}.

Through the data logger, air temperatures, relative humidity and the solar irradiance in the dryer were recorded. The heat and mass transfer in the drying unit results in to weight loss from the samples. This was measured by unloading the black plastic square nets containing the three samples and weighing from the digital balance. Approximately 60 seconds was spent on each weight loss measurement and this was done every 30 minutes in the first 6 hours of drying and then hourly until there was no significant change in the weight of the samples.

The experiments were conducted between 9:00 hours and 16:00 hours on each day of drying due to the abundance of the solar radiation in this period of the day. At the end of a drying day, the mango was packed tightly in polyethylene bags to prevent any moisture loss or gain from the surrounding during the night. Drying was resumed on a following day by unpacking the mango from the polyethylene bags and reloading in to the dryer.

2.4 Natural convection: Buoyant pressure

The difference in air densities inside the dryer and outside (ambient) creates a buoyant pressure head which is the driving force for air in natural convection systems. The buoyant pressure is described mathematically using equation (1) [11-13].

$$\Delta P_b = gH\left(\rho_{am} - \overline{\rho}_{ch}\right) \quad (1)$$

Between air temperatures of 25 and 90 °C, equation (1) was manipulated to yield equation (2) which is in terms of air temperatures [11].

$$\Delta P_b = 0.00308gH\left(T_{ch} - T_{am}\right) \quad (2)$$

Equation (2) was used in this study to calculate the buoyant pressure head.

2.5 Mathematical modelling

From the weight loss measurements, the moisture content was calculated and converted to moisture ratio (MR). MR is mostly calculated according to equation (3), however, a simplified form represented by equation (4) was used to calculate the MR [3, 14, 15].

$$MR = \frac{M - M_e}{M_o - M_e} \quad (3)$$

$$MR = \frac{M}{M_o} \quad (4)$$

M, and M_e are the moisture contents (w.b.) at time t, and equilibrium respectively.

The reason given for the simplification of equation (3) to equation (4) is the exposure of the product in tunnel dryers to varying temperature and relative humidity.

The MR results were fitted into 12 thin layer models in table 1 using the Matlab R2011b curve fitting tool (cftool). The cftool requires a maximum of three input parameters (X data, Y data and Z data). The inputs to the cftool were MR in the Y data and time in the X data. The thin layer equations were entered in to the cftool as custom equations and the best model chosen according to a criteria of three statistical parameters: sum of square error (SSE), coefficient of determination (R^2) and root mean square error (RMSE). In the cftool, the three parameters SSE, R^2 and RMSE are calculated according to equations (5), (6) and (7) respectively.

$$SSE = \sum_{i=1}^{n} w_i \left(MR_{Exp} - MR_{\Pr ed}\right)^2 \quad (5)$$

$$R^2 = 1 - \frac{SSE}{\sum_{i=1}^{n} w_i \left(MR_{Exp} - \overline{MR}Exp\right)^2} \quad (6)$$

$$RMSE = \sqrt{\left(\frac{SSE}{v}\right)} \quad (7)$$

TABLE 1

THIN LAYER MODELS

Model no.	Model Name	Model equation
1.	Newton	$MR = e^{(-kt)}$
2.	Page	$MR = e^{(-kt^n)}$
3.	Modified Page	$MR = e^{(-kt)^n}$
4.	Henderson and Pabis	$MR = a\, e^{(-kt)}$
5.	Logarithmic	$MR = a\, e^{(-kt)} + c$
6.	Two term	$MR = a\, e^{(-k_0 t)} + b\, e^{(-k_1 t)}$
7.	Approximation of Diffusion	$MR = a\, e^{(-kt)} + (1-a)e^{(-kbt)}$
8.	Verma et al.	$MR = ae^{(-kt)} + (1-a)e^{(-gt)}$
9.	Modified Henderson and Pabis	$MR = ae^{(-kt)} + be^{(-gt)} + ce^{(-ht)}$
10.	Two term exponential	$MR = ae^{(-kt)} + (1-a)e^{(-kat)})$
11.	Wang and Singh	$MR = 1 + at + bt^2$
12.	Midilli-kucuk	$MR = ae^{(-kt^n)} + bt$

3 RESULTS AND DISCUSSION

The experiments were conducted using mango as the product under natural conditions typical of Lusaka, Zambia. In total, six sets of solar drying experiments were conducted; three dry run and three with the product. The dry run experiments were done to investigate the attainable drying conditions in the dryer before drying the product.

The initial moisture content of mango was found to be 80 % (w.b.) and was reduced to final moisture contents between 13 and 14 % (w.b.) in 11 hours as shown in the drying curve in figure 2. After 11 hours of drying time, any further drying resulted in no further weight loss, hence these final moisture contents may be considered as the equilibrium moisture contents under the air conditions in the drying unit.

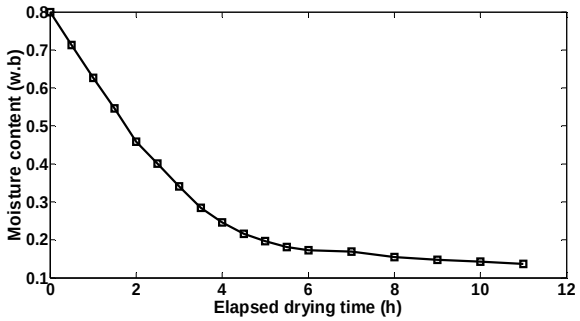

Fig. 2. Mango drying curve

From figure 2, it can be observed that the moisture content decreased continuously with time until the 7th hour of drying. Since the experimental time was between 9:00 hours and 16:00 hours (7 hours) in a day, a continuation of the drying in a following day was inevitable as the product required a total of 11 hours to reach the final moisture content. Therefore, 0 to 7 hours where most of the moisture occurred were on the first day of drying while the last 4 hours were on subsequent day of drying. The final moisture content of mango in this study compared well with final mango moisture contents obtained by Dissa, et al. [16] and Goyal, et al. [3] of 13.79 % (w.b.) and 12 % (d.b.) respectively.

Figure 3 depicts the variation in air temperatures and the solar irradiance in a typical experimental day. The left y-axis represents the air temperatures while the right y-axis represents the solar radiation.

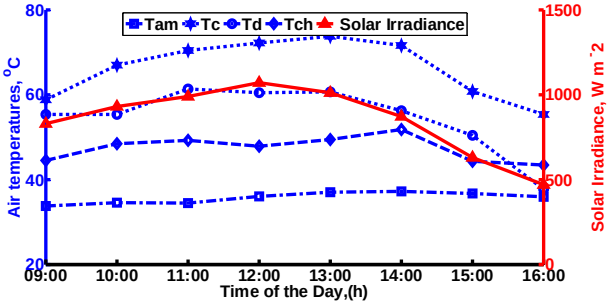

Fig.3. Air temperatures and solar Irradiance on a typical experimental day

The air temperatures, T_c, T_d, and T_{ch} were above T_{am} in ranges of 10-30 °C throughout the day and this implies that the dryer conditioned well the drying air. Similar results have been observed in a tunnel dryer used for drying tomatoes [17]. At the collector unit, air temperature of up to 70 °C was recorded and this dropped after drying the product in the drying unit to an average value of 54. 7 °C.

Air temperature dropped further in the chimney unit by an average of 7.3 °C from the drying unit temperature, however, the air temperatures were kept above ambient by the chimney. The further drop in the air temperature in the chimney unit was not expected. This unexpected phenomena can be explained the high thermal losses and low thermal efficiencies associated with the bare flat-plate type of solar collectors [13]. The advantage of the bare-flat plate chimneys is their simplicity in construction, hence low cost and this makes them suitable for low cost solar drying technologies.

The trend of the air temperatures observed in figure 3 shows that while the solar irradiance reached maximum (1070 W m^{-2}) at around mid-day, the air temperatures T_c, T_d, and T_{ch} were also maximum. As the solar irradiance declined after 14 hours, the air temperatures declined as well, implying a dependence of the air temperatures on the solar irradiance.

The dependence of air temperatures on the solar irradiance was investigated through simple linear regression analysis. The investigation showed a positive correlation between the collector temperature rise above ambient and the solar irradiance with a coefficient of correlation of 0.8865 as shown in figure 4.

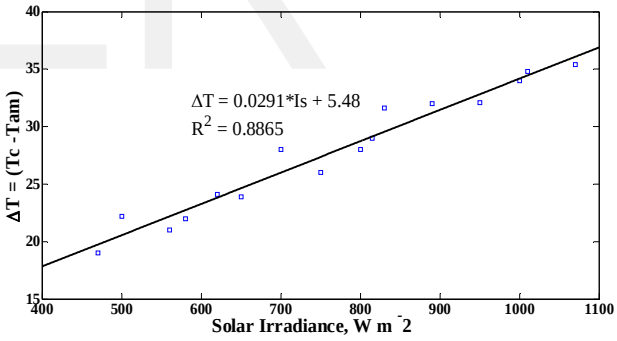

Fig. 4. Temperature rise at the collector exit above ambient

In Hossain and Bala [18], a mean collector temperature rise above ambient of 21.62 °C was registered while this study registered a mean collector temperature rise above ambient of 30 °C which is significantly ($p<0.05$) higher. From figure 4, it is clear that the magnitude of air temperature rise depends on the received solar irradiance, therefore, this can explain any differences in temperature rise between this study and other studies.

The ambient relative humidity varied between 10 % and 30 % and was lowered by over 50 % at the collector unit as shown in figure 5.

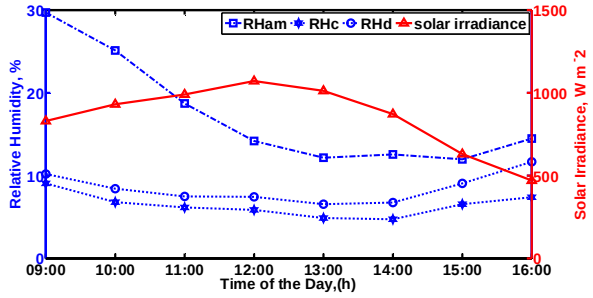

Fig. 5. Relative humidity and solar Irradiance

As observed for the air temperatures, the relative humidity exhibited a dependence on the solar irradiance. The RH_{am}, RH_d and RH_c were lowest at around 13:00 hours and remained fairly low until 15:00 hours where a small increase was observed due to the decrease in the solar irradiance. At the drying unit where the air picks up moisture from the product, the RH_d rose above the RH_c, but was below RH_{am}. The average relative humidity values were 17.3 %, 6.5 % and 8.4 % for $RH_{am,}$ RH_c and RH_d respectively meaning the ambient relative humidity was lowered by over 50 % in the dryer. Therefore, it may be concluded that the dryer performed well in keeping the relative humidity inside the dryer well below ambient even after drying the product. Since the air density is related to the relative humidity, it is worthwhile noting that the observed low relative humidity enhanced the chimney role of generating some magnitude of buoyant pressure.

From the relationship of buoyant pressure head and air temperature in equation (2), the buoyant pressure in the dryer was calculated and was found to range between 0.1530 N m^{-2} and 0.3016 as shown in figure 6.

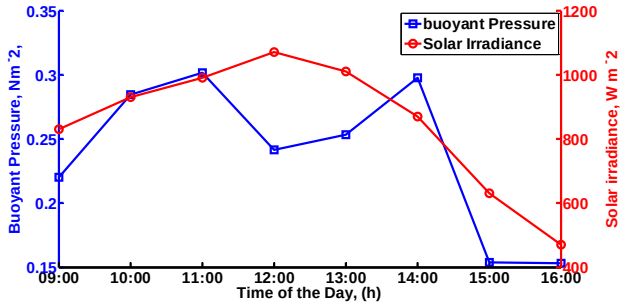

Fig. 6. Buoyant pressure and solar Irradiance

Although the buoyant pressure was relatively low as shown in figure 6, it was sufficient to drive air flow in the dryer. Figure 6 emphasizes the dependence of the conditions in the dryer on solar irradiance as obtained for the air temperature and relative humidity in figures 3 and 5 respectively. The ambient wind velocity and dryer air velocities were on average 0.36 m s^{-1} and 0.04 m s^{-1} respectively implying that the pressure due wind flow was too low and hence, only buoyant pressure was responsible for air flow.

The results from the thin layer modelling are shown in table 2. The model constants and the criteria values; R^2, SSE and RMSE are shown.

TABLE 2

THIN LAYER MODEL RESULTS

Model No.	Best fit Order	Model Coefficients	R^2	SSE × 10^{-3}	RMSE × 10^{-2}
12.	1.	a = 0.9842 b = 0.01614 k = 0.3196 n = 1.072	0.9959	4.634	1.758
8.	2.	a = 0.9565 g = -0.1252 k = 0.3496	0.9953	5.308	1.821
7.	3.	a = 0.9565 b = -0.3585, k = 0.3496	0.9953	5.308	1.821
6.	4.	a = 0.9548 b =0.04172, k_0 = 0.3467 k_1 = 0.1288	0.9953	5.288	1.878
5.	5.	a = 0.8552 b = 0.1524 k = 0.4184	0.9926	8.274	2.274
9.	6.	a = 31.82 b = 0.4129 c = -31.26 g = 0.1052 h = 0.9254 k = 0.915	0.9879	13.619	3.237
3.	7.	k= 0.2764 n = 0.7553	0.9715	32.067	4.343
2.	8.	a = 0.2896 k = 0.6932	0.9715	32.067	4.343
10.	9.	k = 0.3787 n = 0.7553	0.9673	36.771	4.651
11.	10.	a = -0.2268 b = 0.01464	0.9538	51.949	5.528
4.	11.	a = 0.9327 k = 0.2503	0.9489	57.447	5.813
1.	12.	k = 0.2731	0.9404	67.005	6.101

Key. 1. Highest R^2, and lowest SSE and RMSE –Most accurate model

12. Lowest R^2, and highest SSE and RMSE – Least accurate model

From table 2, all the model R^2 values were greater than 0.9 indicating their acceptability[19]. By exploring the SSE and RMSE, only one model was chosen according to the key below table 2. Midilli-Kucuk model qualified as the best fit or most accurate model with parameters; R^2 of 0.9959 (Highest), SSE and RMSE (lowest) of 0.004634 and 0.01758 respectively. To show the goodness of fit by the Midilli-kucuk model, a plot of experimental MR and Midilli-Kucuk model predicted MR against drying time is shown in figure 7.

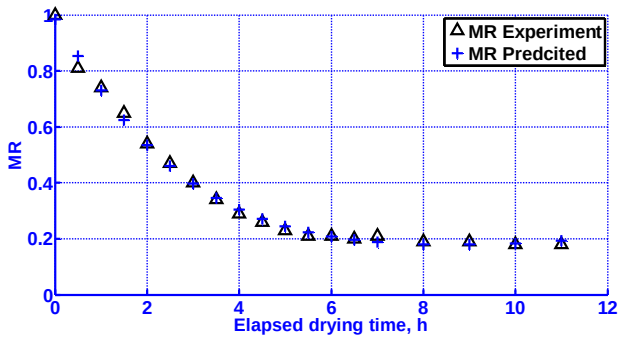

Fig. 7. Experimental and model predicted MR

It can be observed from figure 7 that the experimental and model predicted MR compared well and this validates Midilli-Kucuk model for this study. Goyal, et al. [3] found Page model as the best model to predict drying of raw mango, however, the tunnel dryer used in their study was a forced convection type. Further contrast was in the drying temperatures. Controllable air temperatures of 55, 60 and 65 °C were used in their study whereas this study proceeded under natural air temperatures in figure 3 and under very low air velocities. The ambient air velocity averaged 0.36 m s^{-1} while the air velocity inside dryer was 0.04 m s^{-1}. The cumulative effect of these conditions explain the disparity in models obtained by this study and in [3].

4 Conclusions

In all the drying experiments, the dryer maintained good drying conditions. With a mean solar irradiance of 850 W m^{-2}, the mean collector temperature was 65 °C while the mean RH_c was 6.5 %. However, the air velocities were relatively low implying that the air flow was entirely dependent on the buoyant pressure head. Sufficient buoyant pressure to drive the flow of air in the dryer was developed because the bare flat-plate chimney kept the temperature of the air exiting the drying unit above ambient. Under these conditions, 5 mm mango slices were dried from an initial moisture content of 80 % (w.b.) to between 13 and 14 % (w.b.) in only 11 hours. The results of the thin layer modelling showed that Midilli-Kucuk model best described the drying behavior of mango in the natural convection dryer with an R^2 of 0.9951 and RMSE of 0.01758. In general, the dryer performance was satisfactory and therefore can be deemed suitable for low cost fruit drying applications especially in developing countries such as Zambia.

Acknowledgements

The authors wish to thank Dr. J.M. Chileshe, the Head of Department Agricultural Engineering, University of Zambia and his entire teaching and technical staff for their support during this study. The authors also acknowledge the funding from the European Commission through the METEGA–Intra-ACP Academic Mobility Scheme.

Nomenclature

M	Moisture content at any time, decimal	n	Number of data points
R^2	Coefficient of determination	v	Residual degrees of freedom
SSE	Sum of Square Error	w.b.	Wet basis
RMSE	Root Mean Square Error	d.b.	Dry basis
T	Air temperature, °C	t	Drying time, hours
GI	Galvanized iron sheet		Subscripts
RH	Relative humidity, %	am	Ambient
g	Acceleration due to gravity, m s^{-2}	c	Collector unit
I_s	Solar Irradiance , W m^{-2}	d	Drying unit
H	Chimney height, m	ch	Chimney unit
h	hours	Exp	Experimental Value
ρ	Air density, kg m^{-3}	Pred	Predicted value
$\bar{\rho}$	Mean air densitykg m^{-3}	e	Equilibrium
MR	Moisture Ratio	o	Initial
$\overline{MR}$	Mean MR		

References

[1] R. E. Paull and O. Duarte, Tropical fruits vol. 1: CABI, 2011.
[2] M. A. Leon, S. Kumar, and S. Bhattacharya, "A comprehensive procedure for performance evaluation of solar food dryers," Renewable and Sustainable Energy Reviews, vol. 6, pp. 367-393, 2002.
[3] R. Goyal, A. Kingsly, M. Manikantan, and S. Ilyas, "Thin-layer drying kinetics of raw mango slices," Biosystems Engineering, vol.

95, pp. 43-49, 2006.
[4] İ. T. Toğrul and D. Pehlivan, "Modelling of drying kinetics of single apricot," Journal of Food Engineering, vol. 58, pp. 23-32, 2003.
[5] E. K. Akpinar and Y. Bicer, "Mathematical modelling of thin layer drying process of long green pepper in solar dryer and under open sun," Energy Conversion and Management, vol. 49, pp. 1367-1375, 2008.
[6] E. K. Akpinar, Y. Bicer, and F. Cetinkaya, "Modelling of thin layer drying of parsley leaves in a convective dryer and under open sun," Journal of food engineering, vol. 75, pp. 308-315, 2006.
[7] M. Hossain and B. Bala, "Drying of hot chilli using solar tunnel drier," Solar Energy, vol. 81, pp. 85-92, 2007.
[8] O. Ekechukwu and B. Norton, "Review of solar-energy drying systems III: low temperature air-heating solar collectors for crop drying applications," Energy Conversion and Management, vol. 40, pp. 657-667, 1999.
[9] S. Soponronnarit, W. Subannapong, and J. Tiansuwan, "Studies of Bare and Glass-Cover Flat-Plate Solar Air Heaters," RERIC International Energy Journal, vol. 12, pp. 1-19, 1990.
[10] AOAC, Official methods of analysis. Washington DC: Association of Official Analytical Chemists International 2005.
[11] B. Brenndorfer, L. Kennedy, and G. Mrema, Solar dryers: their role in post-harvest processing: Commonwealth Secretariat, 1987.
[12] W. Grainger, H. Othieno, and J. Twidel, "Small scale solar crop dryers for tropical village use-theory and practical experiences. ISES, Solar World Forum, Brighton, UK," Pergamon Press, Oxford, vol. 1981, pp. 989-96, 1981.
[13] O. Ekechukwu and B. Norton, "Design and measured performance of a solar chimney for natural-circulation solar-energy dryers," Renewable energy, vol. 10, pp. 81-90, 1997.
[14] M. Pala, T. Mahmutoğlu, and B. Saygi, "Effects of pretreatments on the quality of open-air and solar dried apricots," Food / Nahrung, vol. 40, pp. 137-141, 1996.
[15] I. Doymaz, "Effect of pre-treatments using potassium metabisulphide and alkaline ethyl oleate on the drying kinetics of apricots," Biosystems Engineering, vol. 89, pp. 281-287, 2004.
[16] A. Dissa, J. Bathiebo, S. Kam, P. Savadogo, H. Desmorieux, and J. Koulidiati, "Modelling and experimental validation of thin layer indirect solar drying of mango slices," Renewable Energy, vol. 34, pp. 1000-1008, 2009.
[17] K. Sacilik, R. Keskin, and A. K. Elicin, "Mathematical modelling of solar tunnel drying of thin layer organic tomato," Journal of Food Engineering, vol. 73, pp. 231-238, 2006.
[18] M. Hossain and B. Bala, "Thin-layer drying characteristics for green chilli," Drying Technology, vol. 20, pp. 489-505, 2002.
[19] P. S. Madamba, R. H. Driscoll, and K. A. Buckle, "The thin-layer drying characteristics of garlic slices," Journal of food engineering, vol. 29, pp. 75-97, 1996.